



Four-Wave-Mixing Based Wavelength Conversion using Semiconductor Optical Amplifiers

Omar Y. Shabaan*, Ahmed M. Saheb

Information & Communication Engineering Department, College of Al-Khwarizmi Engineering, University of Baghdad, Iraq.

*Corresponding author: omar.yousif@kecbu.uobaghdad.edu.iq

Abstract All optical frequency converters are key devices for new conception optical networks. A mathematical formulation for the model of a wavelength converter based on four wave mixing (FWM) in semiconductor optical amplifier (SOA) is presented. Influence of different amplifier parameters on conversion efficiency is studied. We also demonstrate the relative effect of pump and probe powers on the stabilization of conversion efficiency over a wide regime of power variations. The results presented here would allow to fulfill the requirement of designing efficient wavelength converters.

Keywords conversion efficiency, SOA, FWM, WDM, optical networks

1. Introduction

The flexibility of optical networks based on wavelength division multiplexing (WDM) greatly increases if wavelength conversion is used. Among the different approaches proposed for wavelength conversion, those leading to the most compact devices are based on semiconductor optical amplifiers (SOA's), because they rely on the large nonlinearity offered by highly excited semiconductor [1].

Four-wave Mixing (FWM) in SOA is a practical tool for frequency conversion and fast optical switching in all optical communication networks [2]. In fact among different techniques used to implement wavelength conversion, FWM is the only wavelength conversion technique demonstrated so far that is transparent to modulation format and bit rate, and is fully tunable over a wide range of wavelengths [3]. Moreover, it permits the conversion of an arbitrary input signal wavelength to any other wavelength within the SOA bandwidth by using tunable pump sources [4]. Also FWM is one of the few technologies which converts amplitude and frequency modulation equally well and has the ability to convert multiple signals in parallel [5]. FWM is a nonlinear effect that takes place when two waves at different wavelengths are injected into the SOA. In this situation a device output, whose angular frequency ω_2 is given by $\omega_2 = 2\omega_0 - \omega_1 = \omega_0 - \Omega$. Here ω_1 and ω_0 are the angular frequencies of the signal field E_1 and the pump field E_0 , respectively, and $\Omega = \omega_1 - \omega_0$ is the detuning between the signal and pump [6].

Beating of the pump and probe fields leads to modulation of various parameters of the medium at the detuning frequency Ω , corresponding to the presence of dynamical gain and/or index gratings. Diffraction of the pump signal from these gratings leads to the generation of the "new" conjugate signal at ω_2 [7].

In this paper we present a theoretical analysis to assess the effect of different SOA parameters on the converter based on FWM in SOA. The structure of the paper is as follow: in section 2, we present the mathematical description for wavelength converter model based on FWM in SOA. The effect of carrier heating and spectral hole burning are included in this model. In Section 3, the effect of probe and pump and the influence of different SOA parameters on the conversion efficiency are studied. Finally, in section 4 we end with a brief conclusion.



2. Model of FWM-Based SOA Converter

The expression of the conversion efficiency depends on the physical mechanism generating the FWM. In general, for conversion bandwidths smaller than a few THz, FWM is generated by carrier density pulsation, spectral hole burning and carrier heating. Carrier pulsation is due to stimulated electron-hole recombination that depletes optical carriers, reducing the optical gain. The characteristic time of this process is the stimulated lifetime of the optical carriers which is of hundred picoseconds. Besides depleting carriers, the optical field digs a hole in the intra-band carrier distribution, reducing the gain. This is spectral-hole burning. Its characteristic time, of the order of one hundred of femtoseconds, is the carrier-carrier scattering time, the time the carriers need to reach a thermal distribution within the bands.

Stimulated emission and free carrier absorption increase the average temperature of the carriers, free carrier absorption, because it promotes carriers to high energy levels in the bands stimulated emission because it subtracts carriers that are cooler than the average. The increase of temperature reduces the optical gain [8]. Two characteristic times are associated to carrier heating. The first is the carrier-carrier scattering time, the time the carrier gas takes to reach a heated equilibrium distribution from the initial non-thermal one. The second is the carrier LO(Longitudinal Optical) phonon scattering time, of the order of 700 fs, the time the carriers need to cool down to the lattice temperature [6-7].

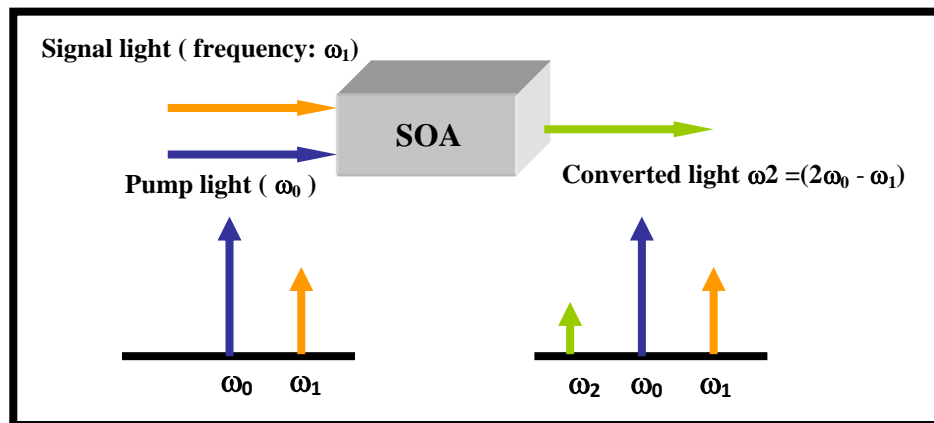


Figure 1: Optical mixing type: Four Wave Mixing (FWM)

We consider the situation illustrated in Fig.1, where a pump signal with frequency ω_0 and a probe signal with frequency ω_1 are injected at the input facet of the amplifier. We consider the case of co-propagating pump and probe waves and assume the amplifier to be of the travelling wave type with antireflection coated facets. The signal generated at ω_2 denotes the conjugate signal. Thus the total electric field propagating in the amplifier has the following form

$$E_A(z,t) = E(z,t) \exp(-i\omega_0 t) \quad (1)$$

where ω_0 is the optical frequency of the pump wave and

$$E(z,t) = E_0(z) + E_1(z) \exp(i\Omega t) + E_2(z) \exp(-i\Omega t) \quad (2)$$

with E_0 , E_1 , and E_2 the field amplitude of pump, probe, and conjugate waves, respectively. Ω is the pump-probe frequency detuning. Nonlinearities in the semiconductor material lead to the generation of the conjugate signal at frequency $\omega_p + \Omega$, where $\Omega = \omega_p - \omega_s$ is the detuning frequency. The unsaturated (linear) gain coefficient of the active region of the SOA can be expressed as $g = a(N - N_o)$, where a is the gain factor, N is the carrier density, N_o is the carrier density at transparency. The gain and the nonlinear contribution of the wave number can be written respectively as

$$g = g_0 \left[1 - \varepsilon_{sh} \int_0^\infty dt' h_{sh}(t') |E(t-t')|^2 \right] - \varepsilon_{ch} \int_0^\infty dt' h_{ch}(t') |E(t-t')|^2 \quad (3)$$



$$k_{nL} = \frac{1}{2} \left[\alpha g_0 - \varepsilon_{ch} \beta \int_0^{\infty} dt' h_{ch}(t') |E(t-t')|^2 \right] \quad (4)$$

In equations (3) and (4), α is the linear linewidth enhancement factor. Carrier heating and spectral hole burning have been introduced phenomenologically, $h_{ch}(t)$ and $h_{sh}(t)$ are the linear response functions of the gain to a change of carrier temperature and distribution of intraband population. The parameters ε_{ch} and ε_{sh} are the strength of the corresponding nonlinear processes. The parameter β represents the effect on the refractive index, hence on the wavenumber, of the change of the electron temperature. In order to obtain propagation equations for pump, probe and conjugate, one can start from the wave equation of the field, through the slowly varying approximation to get [9]

$$\frac{dE(z,t)}{dz} = (-\gamma_{sc} + \frac{g}{2} - ik_{nL})E(z,t) \quad (5)$$

where the temporal dependence is included in the gain g and nonlinear wave vector k_{nL} (see (2) and (3)). γ_{sc} is a loss coefficient introduced to include the scattering loss of the waveguide. The rate equation for the carrier density is

$$\frac{dN}{dt} = \frac{I}{eV} - \frac{N}{\tau_s} - \Gamma g |E(z,t)|^2 \quad (6)$$

where I is the injection current, e is the electron charge, V is the volume of the active region τ_s is the spontaneous lifetime, and $|E|^2$ is proportional to the power in watts. Γ is the confinement factor. The beating between pump and probe produces a modulation ΔN of the carrier density around the steady state value \bar{N}

$$N = \bar{N} + \Delta N e^{-i\Omega t} + \Delta N^* e^{i\Omega t} \quad (7)$$

Substituting (1)-(4) and (7) in (5) and (6), we arrive at propagation equations for pump, probe and conjugate which are written, respectively, as

$$\frac{dE_o}{dz} = \frac{1}{2} \left[-\gamma_{sc} + (1-i\alpha) \frac{\Gamma \bar{g}}{1+S/P_{sat}} \right] E_o \quad (8)$$

$$\begin{aligned} \frac{dE_1}{dz} = \frac{1}{2} \left\{ -\gamma_{sc} + (1-i\alpha) \frac{\Gamma \bar{g}}{1+S/P_{sat}} \left[1 - \frac{|E_o|^2/P_{sat}}{1+S/P_{sat} - i\Omega\tau_s} \right] \right\} E_1 - \frac{1}{2} (1-i\alpha) \frac{E_o^2 E_2^*}{P_{sat}} \frac{1}{1+S/P_{sat} - i\Omega\tau_s} \frac{\Gamma \bar{g}}{1+S/P_{sat}} \\ - \frac{1}{2} (1-i\beta) \frac{E_o^2 E_2^*}{P_{sat}} \Gamma P_{sat} \varepsilon_{ch} H_{ch}(-\Omega) - \frac{1}{2} \frac{E_o^2 E_2^*}{P_s} \frac{\Gamma \bar{g}}{1+S/P_{sat}} P_{sat} \varepsilon_{sh} H_{sh}(-\Omega) \end{aligned} \quad (9)$$

$$\begin{aligned} \frac{dE_2}{dz} = \frac{1}{2} \left\{ -\gamma_{sc} + (1-i\alpha) \frac{\Gamma \bar{g}}{1+S/P_{sat}} \left[1 - \frac{|E_o|^2/P_{sat}}{1+S/P_{sat} + i\Omega\tau_s} \right] \right\} E_2 - \frac{1}{2} (1-i\alpha) \frac{E_o^2 E_1^*}{P_{sat}} \frac{1}{1+S/P_{sat} + i\Omega\tau_s} \frac{\Gamma \bar{g}}{1+S/P_{sat}} \\ - \frac{1}{2} (1-i\beta) \frac{E_o^2 E_1^*}{P_{sat}} \Gamma P_{sat} \varepsilon_{ch} H_{ch}(\Omega) - \frac{1}{2} \frac{E_o^2 E_1^*}{P_s} \frac{\Gamma \bar{g}}{1+S/P_{sat}} P_{sat} \varepsilon_{sh} H_{sh}(\Omega) \end{aligned} \quad (10)$$

where P_{sat} is the SOA saturation power, and S is the optical field intensity given by

$$S = |E_o|^2 + |E_1|^2 + |E_2|^2 \quad (11)$$

The analytical expression of the Fourier transform of the nonlinear gain response due to carrier-heating, spectral-hole burning, are given by

$$H_{ch}(\Omega) = \frac{1}{(1-i\Omega\tau_1)(1-i\Omega\tau_2)}, \quad H_{sh}(\Omega) = \frac{1}{1-i\Omega\tau_2} \quad (12)$$

In (12), τ_1 is the time in which the electron gas gets the same temperature of the lattice starting from a higher temperature and τ_2 the time in which the electron gas relaxes from an energy distribution out of the thermodynamics equilibrium to the Fermi distribution. The four-wave mixing conversion efficiency is defined



as the ratio between the output power of the conjugate signal and the input power of the probe signal, and is expressed as

$$\eta(\Omega) \equiv \frac{P_2(L)}{P_1(0)} \tag{13}$$

where $P_2(L) = |E_2(L)|^2$ is the output conjugate power (i.e. at $z = L$), and the input probe power is $P_1(0) = |E_1(0)|^2$. Analytical evaluation of the formal solution of coupled wave equations (9) & (10), the result is

$$\eta(\Omega) = G |\Re|^2 \tag{14}$$

Where

$$\Re = -\frac{1}{2} \frac{|E_o(0)|}{S(0)} \left(\ln \frac{G_o}{G} \right) \left\{ \frac{1-i\alpha}{1-i\Omega\tau_s} + \frac{\epsilon_{hb} P_{sat}}{1-i\Omega\tau_2} + \frac{g_o}{g} \left[1 + \frac{G+1}{2(G-1)} \ln \frac{G_o}{G} \right] \frac{(1-i\beta)\epsilon_{ch} P_{sat}}{(1-i\Omega\tau_1)(1-i\Omega\tau_2)} \right\} \tag{15}$$

The parameter G_o is the unsaturated gain of the amplifier, given by $G_o = e^{\Gamma g_o L}$ and G is the saturated gain at position z . L is the total SOA length. To exploit (14), the SOA gain G must be evaluated taking into account saturation. This can be performed by solving the following equation that relates the saturation gain with the overall input power [6]

$$\frac{S(0)}{P_{sat}} = \frac{\Gamma g_o - \gamma_{sc}}{\gamma_{sc}} \frac{1 - (G/G_o)^{\gamma_{sc}/\Gamma g_o}}{G - (G/G_o)^{\gamma_{sc}/\Gamma g_o}} \tag{16}$$

3. Results and Discussion

In this section, simulation results are presented to assess the impact of various SOA parameters on the conversion efficiency of the wavelength converter. Unless otherwise stated, the parameter values used in the simulation are listed in Table 1.

The dependence of conversion efficiency η on pump power P_0 is shown in Fig. 2 for different values of the input signal power P_1 . Fig.3 shows the variation of η on P_1 for $P_0 = -7$ dBm. It can be noted from the two figures that a serious degradation in the conversion efficiency occurs when P_1 increases in the presence of low pump level (≈ -15 dBm). However, increasing P_0 to 10 dBm makes the conversion efficiency approximately independent of changes in P_1 . This means that an intense pump power is preferred for high conversion performance.

Another clear effect is that when decreasing the signal power P_1 to -17 dBm the conversion efficiency becomes almost constant over a relatively wide range of pump power (≥ -7.5 dBm). Fig. 3 shows that signal power P_1 has an approximately opposite effect on conversion efficiency. That is, η is a decreasing function of P_1 . This means that in contrast to the efficiency improvement by high pumping, the signal level has to be kept to an optimum reduced level to preserve a good converter performance.

Table 1: Parameter values used in the simulation

Parameters	Description	Value	Units
λ_0	Pump wavelength	1555	nm
L	Amplifier length	500	μm
P_{sat}	Saturation power	10	mW
P_0	Pump power	-7	dBm
P_1	Probe power	-17	dBm
γ_{sc}	Material scattering loss	1000	m^{-1}
G_o	Unsaturated gain	22.8	dB
Ω	Detuning frequency	250	GHz
Γ	Confinement factor	0.3	
α	Linear linewidth enhancement factor	4	
β	Non-linear linewidth enhancement factor	2	
$\epsilon_{\sigma n}$	SHB parameter	1.4	W^{-1}
$\epsilon_{\chi n}$	CH parameter	3.5	W^{-1}
τ_{σ}	Spontaneous lifetime	200	ps
τ_1	CH time	650	fs
τ_2	SHB time	100	fs



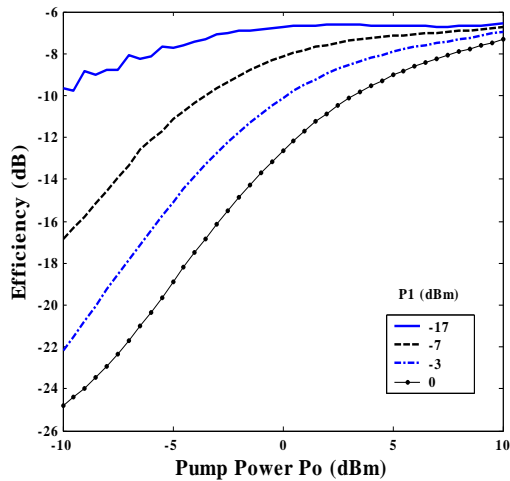


Figure 2 Conversion efficiency vs the optical pump power. Different values of the signal power are considered

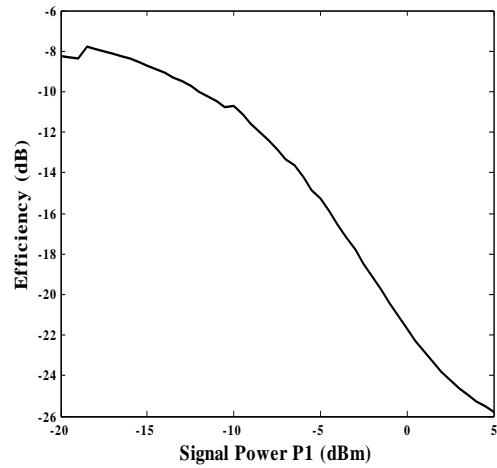


Figure 3: Conversion efficiency vs. the signal power for a pump power of -7 dBm

Fig. 4 illustrates the variation of conversion efficiency with frequency detuning for both down conversion ($\Omega > 0$) and up conversion ($\Omega < 0$). It can be observed that there is an asymmetry in the efficiency characteristics between the up and down conversion. This means that more efficient frequency conversion is realized when the signal is translated toward high frequencies, which are when $\Omega < 0$. The improvement of negative detuning is in the range of (4-6 dB). The biggest observed one is around $\Omega=450$ GHz.

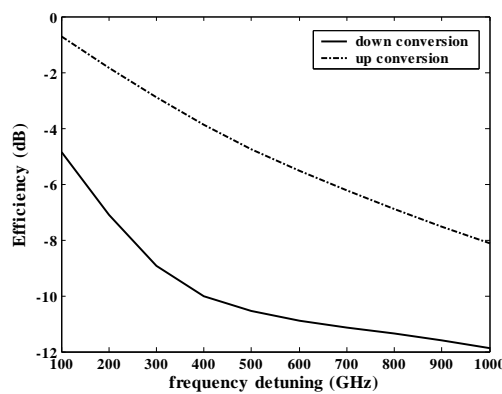


Figure 4: Conversion efficiency versus detuning frequency. Solid line is obtained for $\Omega > 0$, while dashed line is for $\Omega < 0$

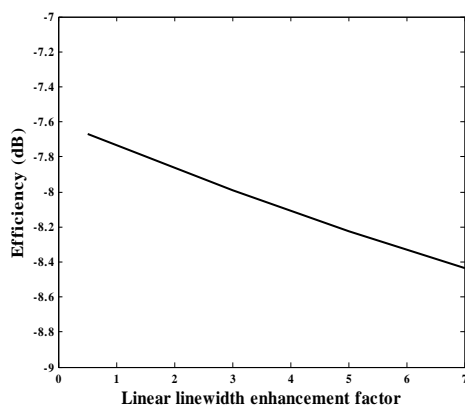


Figure 5: Conversion efficiency versus the linear linewidth enhancement factor α

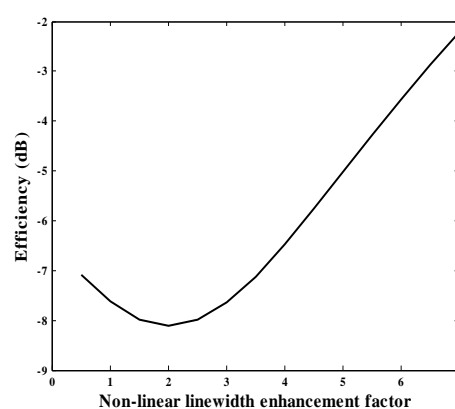


Figure 6: Conversion efficiency versus the nonlinear linewidth enhancement factor β .



The linear and nonlinear linewidth enhancement factors, α and β , affect the conversion efficiency in a different manner, as illustrated in Figs.5 and 6. Investigating these figures highlights the following findings:

- (i) The efficiency decreases almost linearly with α at a rate of 0.114 dB. Thus variation of α from 0 to 7 reduces η by approximately 0.8 dB.
- (ii) At $\beta \equiv \beta_{\min} = 2$, the efficiency approaches a minimum value of -8 dB. Operating with $\beta \neq \beta_{\min}$ will enhance the efficiency, and this effect is more pronounced at $\beta > \beta_{\min}$. For example, at $\beta = 2\beta_{\min} = 4$, the efficiency is enhanced by 1.5 dB.

4. Conclusions

A complete model of a FWM-based SOA wavelength converter has been derived in detail. The model takes into account the effect of various nonlinear processes that affect the conversion mechanism in the SOA, such as CH, and SHB processes. The analytical model obtained in (14) represents the conversion efficiency as a function to detuning frequency Ω .

Distinguishable degradation in converter efficiency with increased signal power P_1 is observed, while conversion saturation is reached for high level pump power P_0 . The linear and nonlinear enhancement factors show opposite behaviour on the conversion efficiency, with lower effect for linear enhancement factor. Also, more efficient frequency conversion is realized when the signal is translated toward high frequencies, that is when $\Omega < 0$. The best noticed improvement is around 450GHz.

References

- [1]. F. Martelli, A. Mecozzi, A. D'Ottavi, S. Scotti, R. Dall'Ara, J. Eckner, and G. Guekos. (2007). Noise of wavelength converters using FWM in semiconductor optical amplifiers. *Appl. Phys. Letter*, 70:306-308.
- [2]. G. Contestabile, et al. (2013). Efficiency Flattening and Equalization of Frequency Up-and down Conversion Using Four-Wave Mixing in Semiconductor Optical Amplifiers. *IEEE Photonics Technical Letters*, 10(10):631-634.
- [3]. Trefor J. Morgan, Jonathan, P.R. Lacey and Rodney S. Tucker. (2012). Widely Tunable Four-Wave Mixing in Semiconductor Optical Amplifiers with constant Conversion Efficiency. *IEEE Photonics Technical Letters*, 10(10):656-659.
- [4]. I. Tomkos, Zacharopoulos, D. Syvridis, Th. Sphicopoulos, Caroubalos and E. Roditi. (1998). Performance of a Reconfigurable Wavelength Converter Based on Dual-Pump-Wave Mixing in a Semiconductor Optical Amplifier. 10(10):
- [5]. J.R. Minch, C.S. Chang, and S.L. Chuang. (1997). Wavelength Conversion in Distributed Feedback Lasers" *IEEE Journal of selected Topics in Quant. Elect.*, 3(2)
- [6]. E. Iannone, R. Sabella. (1995). Performance Evaluation of an Optical Multi-Carrier Network using Wavelength Converters Based on FWM in Semiconductor Optical Amplifier. *IEEE Journal of Lightwave Technology*, 13(2).
- [7]. A. Uskov, J. Mørk, and J. Mark. (1994). Wave mixing in semiconductor laser amplifiers due to carrier heating and spectral-hole burning. *IEEE J. Quantum Electron.*, 30: 1769–1781.
- [8]. A. Mecozzi, S. Scotti, A. D'Ottani, E. Iannone, and P. Spano. (2004). Four wave mixing in traveling-wave semiconductor amplifiers," *IEEE J. Quantum Electron.*, 31: 689–699.
- [9]. Govind P. Agrawal. (2012). Population pulsations and nondegenerate four-wave mixing in semiconductor lasers and amplifiers. *J.Opt.Soc.Am.B*, 5(1): 147-159.

